DEVELOPMENT OF AN EDUCATIONAL SAR PROCESSOR WITH SCANSAR IMAGE FORMATION

Yosuke Ito*[1] , Yuuhei Teramoto[2] and Kenji Abe[3]
[1]Professor, Naruto University of Education
748 Takashima, Naruto-city, Tokushima Pref. 772-8502, Japan
E-mail: ito@naruto-u.ac.jp

[2]Director and [3]Chief Development Officer, Ateral, Inc., 309 Tokushima Science Center 209-5,
Hiraishi-Sumiyoshi, Kawauchi-cho, Tokushima-city, Tokushima Pref. 771-0134, Japan
Email: [2]tera@ateral.com, [3]abek@ateral.com

KEY WORDS: SAR processor, Scan mode, Strip mode, Range-Doppler algorithm, Image formation.

ABSTRACT: Recent spaceborne synthetic aperture radar (SAR) sensors have a variety of sensing modes, including strip, scan, and spotlight modes, for multipurpose observation. Understanding the basic algorithm of SAR image formation is necessary in order to develop new approaches using advanced sensing modes. The SAR with the scan mode (ScanSAR) is particularly useful for sensing a vast area within a limited observation time. Raw SAR data obtained by the strip mode are generally processed by the range-Doppler algorithm. On the other hand, the SPECAN algorithm is applied to process the raw ScanSAR data in consideration of computing efficiency. Each algorithm processes the raw data in a different image coordinate system. In the present study, the image formation algorithm for both strip and scan modes are integrated in order to comprehensively clarify the SAR processing technique. The present paper introduces an educational SAR processor with ScanSAR image formation using the range-Doppler algorithm. Since the ScanSAR repeatedly illuminates several types of beam pulses with different off-nadir angles, range gate times, and pulse repetition intervals. The areas that are not radar illuminated are padded by zero data and the range-compressed data are interpolated along the azimuth direction in order to unify the pulse repetition intervals before azimuth compression. The principle of ScanSAR image formation is clearly indicated by showing all of the intermediate images of the ScanSAR data in the manner same as for strip mode processing. As a web-based application with intuitive operations, the developed processor can produce a focused image with slant range coordinate from the raw SAR data obtained by ALOS PALSAR, ERS-1/2 AMI, RADARSAT-1, and JERS-1 SAR. Orthorectified images are also generated from the focused image based on the specified map projection, DEM, and geoid model. Practical operation and images obtained by the educational SAR processor are demonstrated.

1. INTRODUCTION

Spaceborne synthetic aperture radar (SAR) has been used to observe almost the entire surface of the Earth in order to provide dynamic information to research areas such as vegetation mapping and monitoring, hydrology, sea-ice mapping, and geology. Recently, SARs with strip, scan, and spotlight modes have become available for multipurpose observation. Understanding the basic algorithm of SAR image formation is necessary in order to develop new approaches using advanced sensing modes. Since the release of spaceborne SARs with scan modes, such as RADARSAT-1/2, ALOS PALSAR, and ENVISAT ASAR, the wide-swath SAR images have become more popular. ScanSAR interferometry is also applied for topographic mapping or surface change monitoring in vast areas. The SAR with the scan mode (ScanSAR) is particularly useful for sensing a wide range area within a limited observation time. Raw SAR data obtained by the strip mode are generally processed by the range-Doppler algorithm. On the other hand, the SPECAN algorithm is used to process the raw ScanSAR data in consideration of computing efficiency (Cumming, 2005). In the present study, the image formation algorithm for both the strip and scan modes are integrated in order to understand the SAR processing technique comprehensively. In the present paper, we introduce an educational SAR processor that performs ScanSAR image formation using the range-Doppler algorithm.

2. EDUCATIONAL SAR PROCESSOR

2.1 Specifications

The educational SAR processor was developed in order to facilitate understanding of raw SAR data processing and the sensing scheme (Teramoto, 2009). The software, which is developed as a web-based SAR processor with intuitive operations, can produce a focused image with slant range coordinate from the raw SAR data observed using both the strip and scan modes. The principle of ScanSAR image formation is easily illustrated using intermediate images of the ScanSAR data, in the manner same as the strip mode processing. Since the ScanSAR repeatedly illuminates several

types of beam pulses with different off-nadir angles, range gate times, and pulse repetition intervals (PRIs), the areas that are not radar illuminated are padded by zeros, and the range-compressed data are interpolated along the azimuth direction in order to unify the PRIs before the azimuth compression (Bamler, 1996).

Intermediate complex data produced by focusing the raw SAR data can convert a set of grayscale images. Data arrangement along the range direction is essential in SAR processing. The illuminated beam pulses are received after the range gate time, which is determined according to the slant range. The ScanSAR provides a wide swath by changing the off-nadir angle for each beam. The beam pulses in the scan mode are received after the individual range gate time. The areas for which no signals are received are padded by zero data so as to identify the arrangement of bursts for each beam at a glance. In the general SAR system, one of the available PRIs is chosen according to the slant range. Each beam of the scan mode has a different PRI because the slant range varies remarkably from the near range to the far range. It is necessary to interpolate the complex data along the azimuth direction in order to unify the specified PRI for processing raw SAR data with several types of PRIs. The received signals become invalid after changing the off-nadir angle of the beam. These data must be forced to be zero before azimuth compression. Azimuth compression in the scan mode is normally performed using a single beam. When the Doppler frequency continues at the scan boundary, the area in which the two beams overlap along the azimuth direction exhibits a double bandwidth and produces higher resolution than the area with a single beam. The processor can be set to use the beams in the azimuth compression in various manners. As a post-process, orthorectified images are also generated from the focused image based on the specified map projection, DEM, and geoid model (Ito, 2010).

2.2 Procedure of SAR Image Formation

Figure 1 shows a flowchart of SAR data processing by the range-Doppler algorithm. The procedures consist of six steps. Parameter, data, and log files for the educational SAR processor are newly generated in each step. Either the entire region or a partial region in the data file can be converted to BMP and CSV formats using the corresponding parameter file. Therefore, the learner can review the intermediate images in each step and evaluate the data profile by simply drawing a graph. The applicable raw SAR data for the developed processor are shown in Table 1. The ScanSAR image formation can be applied to RADARSAT-1 and PALSAR data only. An outline of each step of the procedure is shown below.

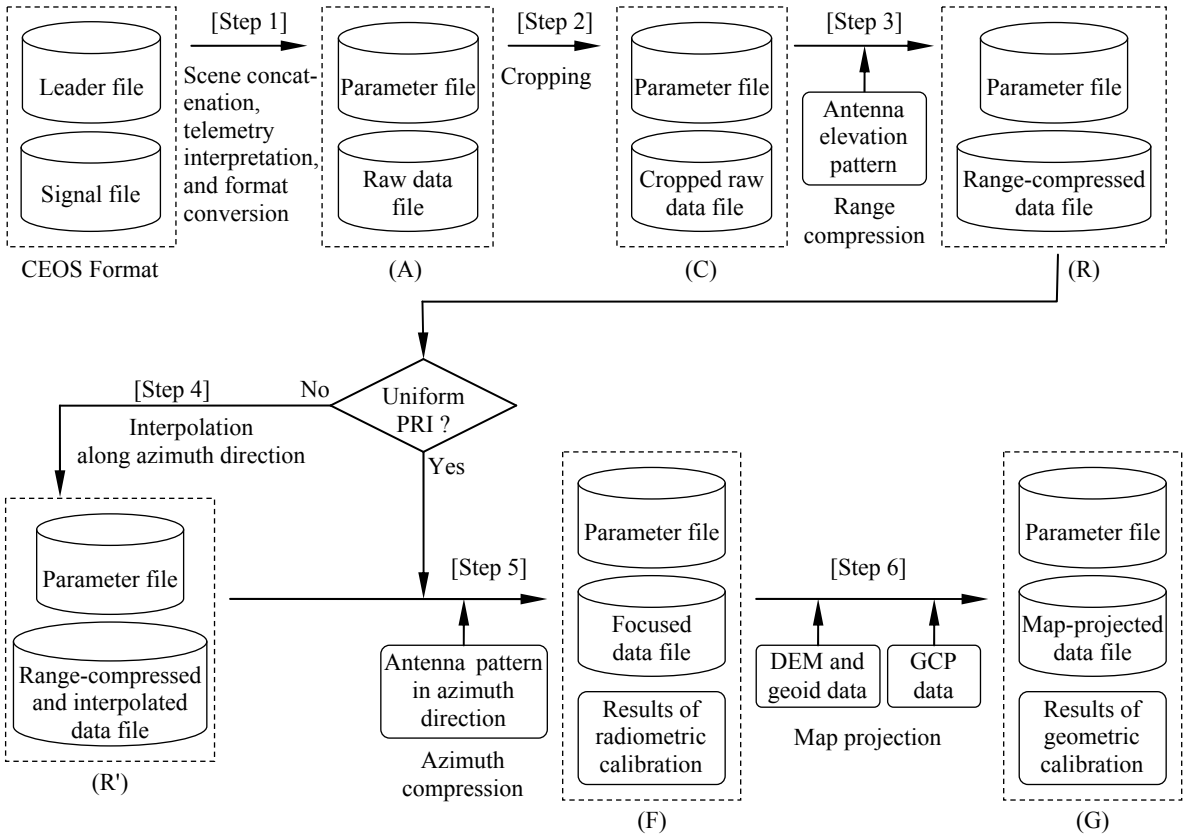

Figure 1. Flowchart of the range-Doppler algorithm for processing both strip and scan SAR data.

In Step 1, the leader and signal files with the Committee on Earth Observation Satellites (CEOS) produced by a SAR data provider are converted to parameter and data files (A) for the educational SAR processor. In the case of processing consecutive scenes in a single operation, these signal files, are in the CEOS format, are concatenated by the developed auxiliary software. Indispensable parameters for focusing the raw SAR data are also estimated and computed based on the telemetry interpretation. Since the parameters are stored in either binary or plain text format in the source files with the CEOS format, the format of the parameter files is plain text with a hierarchical structure. This facilitates the confirmation and changing values in the parameter file. Data such as an estimated Doppler centroid, PRIs, number of beams, locations (latitude and longitude) at the four corners and the center are included in the parameter file (A). The fixed record length in the data file consists of the header and the data sections. The record header includes important parameters, such as detailed observation status stored in a signal file according to the specific format for the individual SAR sensor, the micro-second-order observation time, the mean and standard deviation of the I and Q elements in the record, the beam number, the number of delayed pulses, the valid flag of the received signal, the number of received signals, the number of padded data outside the received signals. If the observation time does not have micro-second-order precision (for example, JERS-1 SAR), then the observation time in each record is estimated by the least squares method. The range gate time from transmitting the pulse to receiving the backscattered signal depends on the location of SAR and the illumination angle of the beam. Thus, the zero data are padded outside the received data in order to adjust the slant range to be the same throughout the entire scene.

The next operation is to crop the raw data file according to the region of interest in Step 2. The parameter file (C) is generated by adding cropping parameters to the parameter file (A). The cropped raw SAR data file (C) is also generated by cropping the entire raw data file (A). The data file can be also cropped for each beam in the scan mode. In Step 3, the parameter and data files (R) are generated by applying the range compression to the parameter and raw data files (C). The range reference function is convolved into the raw SAR data in each range line. Note that there are various options, such as the length of the FFT, the type of window function (including a Kaiser window with α), the degree of filtering to eliminate interference noise from the ground, and secondary range compression. Radiometric distortion caused by applying a window function and the antenna elevation pattern (AEP) is compensated. The AEP data indicate the sensitivity of the antenna for look angles. These values are computed for each beam and polarization based on the results obtained for an area with homogeneous scatter, such as the Amazon rainforest, such that γ^0= -6.5 [dB] (Shimada, 2009). A set of AEP data for each beam is required in the scan mode. An incomplete convolution area occurs at the end of the far range because the range-compressed signal is located at the end of the near range. The incomplete area is usually removed. However, objects in the incomplete area can be recognized by eye, and this area weakly includes the phase information. Therefore, the processor can keep or remove the incomplete area according to the wishes of the operator. Range compression can be performed in parallel processing using the specified number of threads.

Several types of PRIs in the scan mode are used. The strip mode often changes the PRI as well. It is necessary to interpolate the complex data along the azimuth direction in order to unify the specified PRI. In Step 4, the parameter and data files (R') are generated by interpolating the complex data in the range-compressed data file (R). The interpolator adopts the sinc function by default. The digitized precision of the sinc function and the number of points for the interpolation are specified in consideration of the balance between the computational cost and the precision of interpolation. The nearest neighbor method is also used to check the time sequence in the data file. After changing the beam in the scan mode, the lines become invalid because no effective signals are received. The number of invalid lines is the same as the number of delayed pulses. These invalid lines are padded with zeros in Step 4. The interpolator does not use the data received from the different beam.

In Step 5, the parameter and focused data files (F) are generated by applying the azimuth compression to the parameter and the range-compressed data files (R or R'). In the azimuth compression, the Fourier transform in the

Table 1. Applicable SAR data.

Satellite	Sensor	Band	Observation Mode	Polarization
ERS-1/2	AMI	C	Strip mode	VV
JERS-1	SAR	L	Strip mode	HH
RADARSAT-1	SAR	C	Strip mode (Standard beam, Fine beam, Wide beam)	HH
			Scan mode (Narrow beam, Wide beam)	
ALOS	PALSAR	L	Strip mode (Fine beam single pol. (FBS))	HH or VV
			Strip mode (Fine beam dual pol. (FBD))	HH+HV or VV+VH
			Strip mode (Quad pol. (PLR))	HH+HV+VH+VV
			Scan mode (Short burst (WB1) , Long burst (WB2))	HH or VV

azimuth direction is applied to the range-compressed data. The complex data in the frequency domain are interpolated using the sinc function for compensating the range cell migration, where the digitized precision of the function and the number of points for interpolation can be specified as described in Step 4. The azimuth reference function computed at each range is convolved into interpolated complex data. There are various options for the number of looks, the length of the FFT, the type of window function (including the Kaiser window with α), and the processing method in the beam overlapping area. The number of looks should be set to 1 in order to preserve the phase information. Radiometric distortion caused by applying the window function and the antenna pattern in the azimuth direction (AAP) is compensated. The AAP data is mainly used to eliminate the scalloping noise in the scan mode. A set of AAP data for each beam is required in the scan mode. The focused image is corrected so as to continue the intensity at the beam boundary. An incomplete convolution area occurs at both sides in the patch because the azimuth-compressed signal is located at the center. The incomplete area is dealt with in the same manner as Step 3. The azimuth compression can be performed in parallel processing using the specified number of threads. In general, the azimuth compression in the scan mode is performed in each beam. The processor can convolve the area in which the two beams are overlapped. The overlapped area includes wider Doppler bandwidth. The scalloping noise is reduced by introducing the compensation method considering the burst length in the synthetic aperture time. There is no deskew operation by which to generate the zero-Doppler data in order to maintain the original coordinate.

In Step 6, the UTM projection is used only in the educational SAR processor. The data is interpolated by the nearest neighbor method. The parameter and data files (G) are generated by map-projecting the specified ground resolution to the parameter and focused data files (F). A digital elevation model (SRTM-3, ASTER GDEM, ASTER on-demand DEM provided by the GEO Grid (http://www.geogrid.org/), GSI-DEM) and a geoid height model (EGM-96, GSIGEO 2000) can be used for the map projection and the geometric calibration. The geometric error is also calculated using the GCP data. In addition, the map projection is applied for the parameter and data files (C, R, R') in the same manner.

3. PROCESSING EXAMPLES

3.1 ScanSAR Image Formation

ScanSAR image formation using the educational SAR processor is demonstrated. The ScanSAR data observed by ALOS PALSAR with the scan mode includes the backscatter from the Amazon rainforest. The focused image and the detailed sensing information are shown in Figure 2. Figure 3 shows the intermediate images from Step 1 to Step 5 in Figure 1. The processed area is part of the ScanSAR image with the slant range coordinate shown in Figure 2. Figure 3(a) shows the raw ScanSAR image padded with zero data in both the near and far range sides of each beam, so as to unify the range gate time virtually. The learner confirms the sensing locations corresponding to the beams and the burst cycle (L_a) in the scan mode. The time interval in the azimuth direction is changed each burst because the scan mode of PALSAR adopts an individual PRI in each beam. Next, the image for which the range compression is applied to the adjusted raw SAR data is shown in Figure 3(b). Figure 3(c) shows an enlargement of area A1, including beam Nos. 1 and 2. After changing the beam, the learner can clearly identify the invalid lines between the bursts. The number of invalid lines is 12. Figure 3(d) shows the image interpolated along the azimuth direction in order to unify the PRI, which is set to the narrowest interval in each beam in order to maintain as much of the original information as possible. Interpolation is performed using 16 points of the sinc function so as not to add inappropriate elements. Figure 3(e) is an enlargement of area A2, which includes beam Nos. 1 and 2. In the interpolation process, the zero data are also padded in the invalid lines. Finally, Figure 3(f) shows the focused image with single-look complex data. In the case of using the yaw steering mode in PALSAR, the Doppler centroid is assumed to be continuous

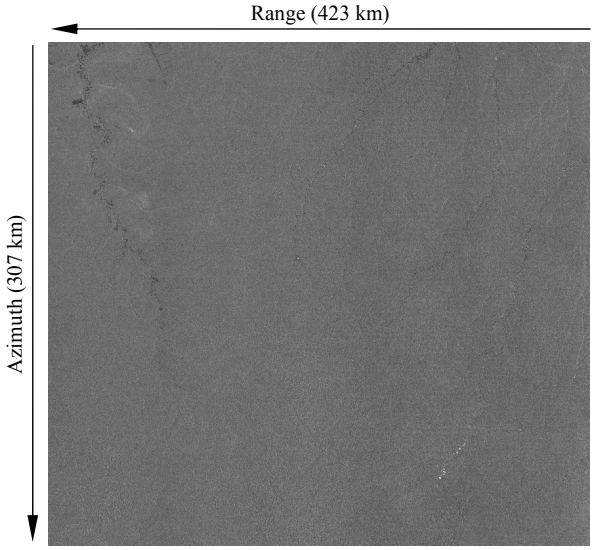

Figure 2. ScanSAR image obtained by ALOS PALSAR (Mode: WB1, Number of beams: 5, Date: 16 April 2007, Center location: 9° 23' 57" S, 71° 54' 9" W, Amazon rainforest, Descending orbit).

between the beams. The valid image is located around the scene center in the azimuth direction. The incomplete compression areas in both sides are padded by the zero data. The synthetic aperture time is set to $3T_s$ such that the illumination period during every three bursts is less than T_s. The scalloping noise in Figure 3(f) is not conspicuous. As a result, the educational SAR processor is shown to be useful for clarifying the ScanSAR image formation by confirming the intermediate images in each procedure.

3.2 Comparison of Processed ScanSAR Images

Figures 4(a) and 4(b) show the map-projected ScanSAR images processed by the range-Doppler and the SPECAN

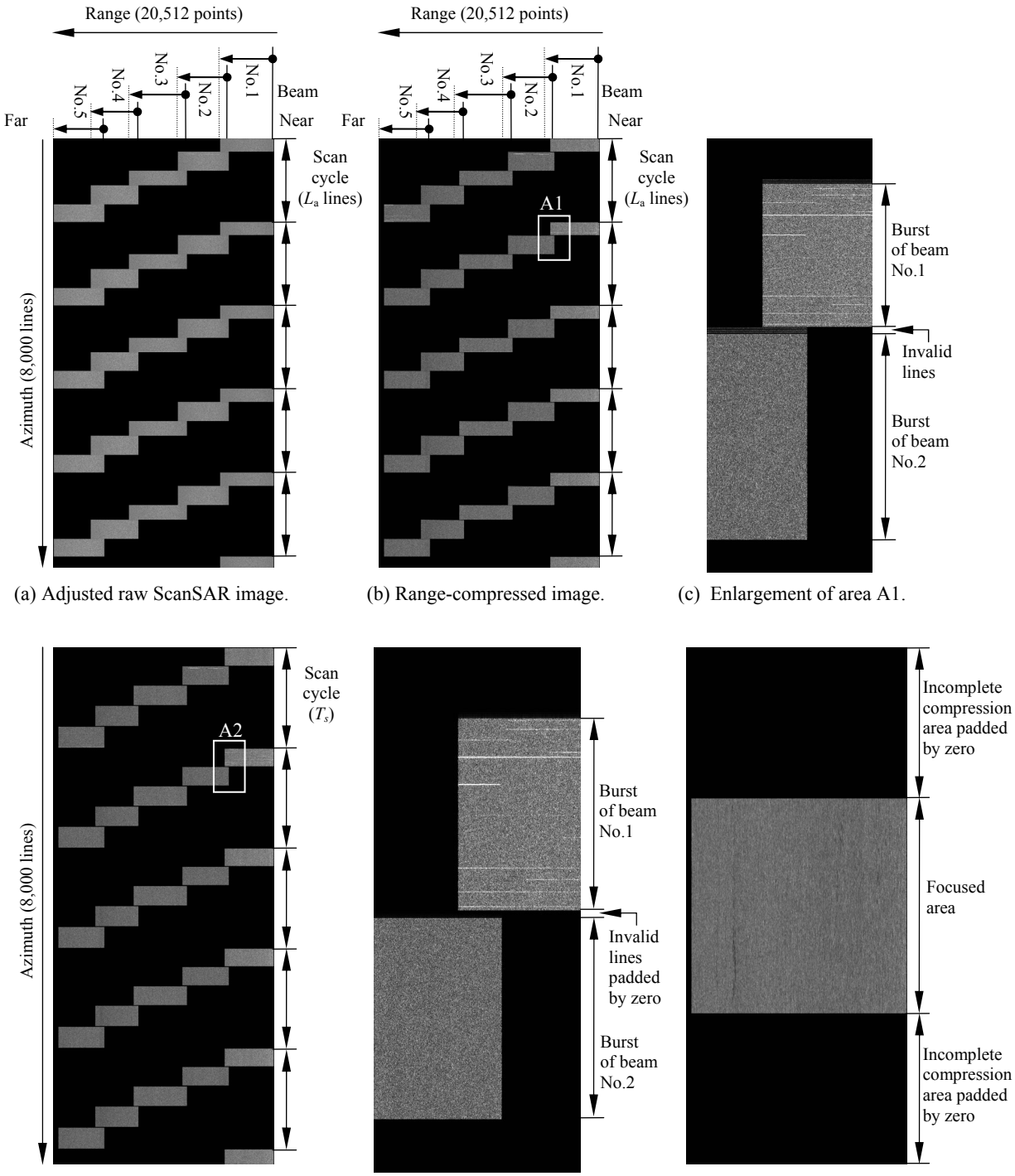

(a) Adjusted raw ScanSAR image.

(b) Range-compressed image.

(c) Enlargement of area A1.

(d) Range-compressed and interpolated image with uniform PRI.

(e) Enlargement of area A2.

(f) Focused image with single-look.

Figure 3. Intermediate images in the ScanSAR image formation.

algorithms, respectively. Since the parameters transforming σ^0 to the grayscale in the SAR images are not equivalent, the contrast and the intensity in these images differ slightly. On the other hand, geometrically, the ScanSAR images are approximately equivalent. In addition, the intensity discontinuity around the beam boundaries in the ScanSAR image is reduced by appropriately compensating the AEP, as shown in Figure 4(a).

4. CONCLUSIONS

The specifications of the educational SAR processor with the ScanSAR image formation were described, and the processing diagram of the developed processor and examples of actual SAR data were presented. The learner can intuitively understand the sensing scheme of the scan mode and the ScanSAR image formation algorithm in a manner similar to the SAR data processing in the strip mode by using the developed processor. Improvement of the core software is planned in order to produce ScanSAR images with more accurate phase information and no scalloping noise for the interferometric SAR processing.

ACKNOWLEDGMENTS

The educational SAR processor uses the outcome of the research commission of the National Institute of Advanced Industrial Science and Technology in Japan. The SAR data were provided under the second ALOS research announcement of the Japan Aerospace Exploration Agency.

REFERENCES

Bamler, R. and Eineder, M., 1996. ScanSAR processing using standard high precision SAR algorithms, IEEE Transactions on Geoscience and Remote Sensing, Vol.34, No.1, pp.212–218.
Cumming, I. G. and Wong, F. H., 2005. Digital Processing of Synthetic Aperture Radar Data, Artech House, Norwood, MA, pp.369–423.
Ito, Y., Teramoto, Y., and Abe, K., 2010. Development of a visual SAR processor and its calibration function, Proceedings of the 31st Asian Conference on Remote Sensing, DVD–ROM.
Shimada, M., Isoguchi, O., Tadono, T., and Isono, K., 2009. PALSAR radiometric and geometric calibration, IEEE Transactions on Geoscience and Remote Sensing, Vol.47, No.12, pp.3915–3932.
Teramoto, Y., Ito, Y., and Abe, K., 2009. Web application system with synthetic aperture radar image processing for education, Transactions Electronics, Information and Systems, IEEJ, Vol.129-C, No.9, pp.1759-1767 (in Japanese).

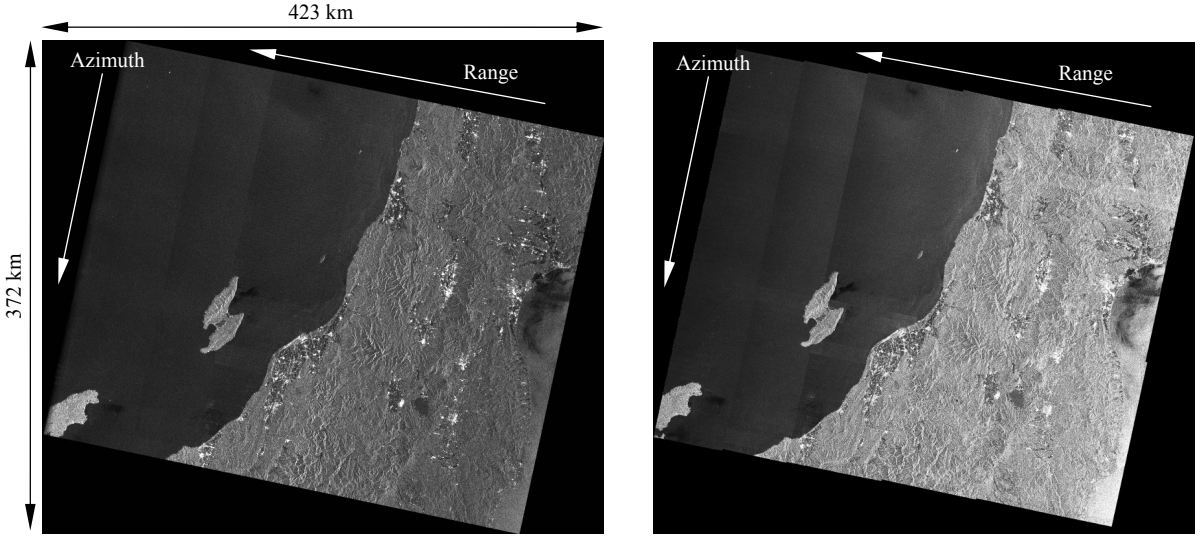

(a) ScanSAR image processed by the educational SAR processor with the range-Doppler algorithm.

(b) ScanSAR image processed by the SPECAN algorithm. The data is provided from ERSDAC as Level 4.2.

Figure 4. Comparison of ScanSAR images processed by different algorithms. The image with σ^0 is projected by UTM. The raw ScanSAR data was obtained by ALOS PALSAR (Mode: WB1, Number of beams: 5, Date: 4 July 2006, Center location: 38° 19' 49" N, 138° 53' 45" E, Niigata, Japan, Descending orbit).